

Chapter 6: Dynamic *O*-Glycosylation Regulates CREB-Mediated Neuronal Gene Expression and Memory Formation

Portions of this chapter are from Clark, P.M., Rexach, J.E., Mason, D.E., Neve, R.L., Peters, E.C. & Hsieh-Wilson, L.C. Regulation of Neuronal Gene Expression and Memory Formation by Dynamic Glycosylation. *Submitted* (2010).

***O*-Glycosylation of proteins with *N*-acetyl-D-glucosamine (*O*-GlcNAc) is an abundant post-translational modification that shares key features with protein phosphorylation; however, its precise functions in the brain are not well understood. We show that *O*-GlcNAc glycosylation regulates cAMP-response element binding protein (CREB), a transcription factor critical for neuronal activity-dependent gene expression, neuronal development, and long-term memory storage. Glycosylation of CREB was dynamically induced by membrane depolarization and repressed CREB-dependent transcription by impairing the association of CREB with the CREB-regulated transcriptional co-activator (CRTC/TORC). Blocking glycosylation of CREB at a single amino acid site promoted axonal and dendritic growth and enhanced long-term memory consolidation. Our studies reveal that *O*-GlcNAc glycosylation plays a major role in essential neuronal processes and higher-order brain functions.**

Dynamic *O*-GlcNAc glycosylation of intracellular proteins is emerging as a crucial regulatory post-translational modification¹⁻⁵. Attachment of this simple glycan, *N*-acetylglucosamine (GlcNAc), to serine or threonine residues occurs on more than 1,000 proteins, including transcription factors, translational regulators, cytoskeletal components, and other nucleocytoplasmic proteins^{1-3,6}. The fact that *O*-GlcNAc glycosylation shares key features with protein phosphorylation, which regulates neuronal processes such as cell signaling, synaptic plasticity, and learning and memory⁷, suggests similar, critical roles for *O*-GlcNAc in the brain. Moreover, several studies have linked *O*-GlcNAc to various neuropathologies, particularly Alzheimer's disease^{1-3,8,9}. Despite

this intriguing body of evidence, little is known about the specific contributions of *O*-GlcNAc to fundamental neuronal functions. Thus, there is a strong rationale to explore how site-specific protein *O*-glycosylation may serve as a critical regulator of higher-order brain function.

To determine specific roles for *O*-GlcNAc in the nervous system, we examined glycosylation of CREB, a transcription factor important for neuronal development and survival, circadian rhythms, drug addiction, and long-term memory consolidation¹⁰⁻¹⁴. Jessica Rexach chemoenzymatically labeled proteins with terminal GlcNAc sugars with a 2,000-Da polyethylene glycol (PEG) mass tag and immunoblotted with an anti-CREB antibody to visualize the glycosylated species (**Fig. 1**). We found that a large fraction of CREB (44–48%) was mono-glycosylated in both cultured cortical neurons and various brain regions of adult mice. To map the glycosylation sites, I transiently expressed CREB in neuro2a cells, immunoprecipitated it, and subjected it to electron transfer dissociation mass spectrometry (ETD-MS) analysis. In addition to the three sites initially identified (Thr259, Ser260, Thr261)¹⁵, *O*-GlcNAc glycosylation was mapped to Ser40 and Thr227 or Thr228 within the Q1 and Q2 domains (**Figs. 2, 3**). Jessica found that expression of a mutant form of CREB, in which Ser40 was mutated to alanine (S40A), led to a large reduction in CREB glycosylation levels in cortical neurons (56%), whereas mutation of both Thr227 and Thr228 (TT227-8AA) led to a smaller decrease in glycosylation (36%; **Fig. 4**). CREB was also glycosylated within Thr259, Ser260, and Thr261 at low levels (TST259-61AAA; 13%), and simultaneous mutation of all six sites (A6) abolished the glycosylation of CREB. These results demonstrate that CREB is

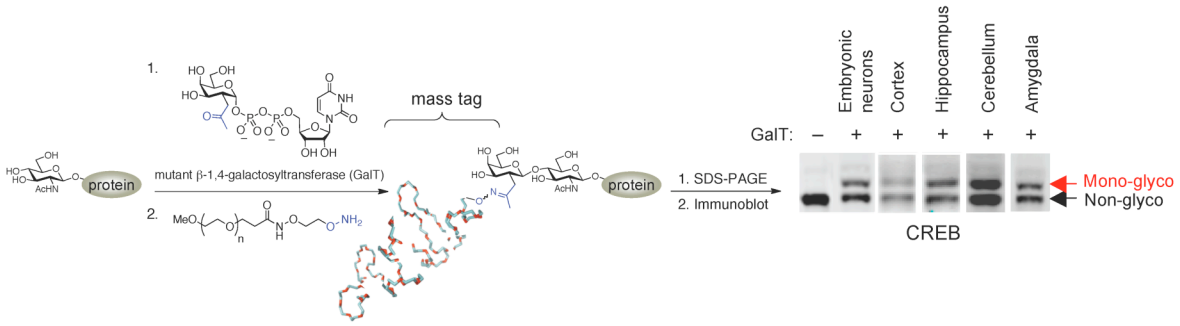


Figure 1: CREB is *O*-GlcNAc glycosylated in neurons. Detection of *O*-GlcNAc glycosylated CREB in neurons by chemoenzymatic labeling with a 2000-Da mass tag

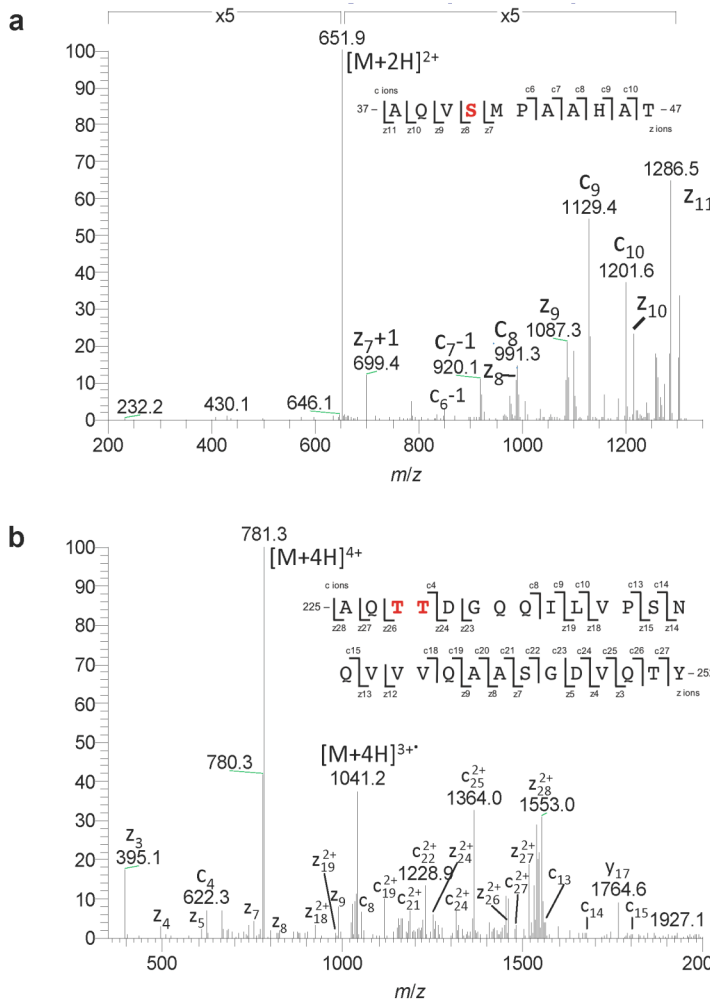


Figure 2: CREB is *O*-GlcNAc glycosylated at Ser40 and Thr227 or Thr228. Mass spectrum of chymotrypsin digested FLAG-CREB from Neuro2a cells. Electron transfer dissociation mass spectrometry (ETD-MS) was performed on the m/z 651.9 ion (a) and the m/z 781.3 ion (b). Shown are annotated spectra for two peptides identified to contain the *O*-GlcNAc modification. The c and z fragment ions observed were used to map the glycosylation sites to the residues indicated

highly glycosylated in neurons, identify all major glycosylation sites on neuronal CREB, and establish Ser40 as the predominant site of *O*-GlcNAc glycosylation.

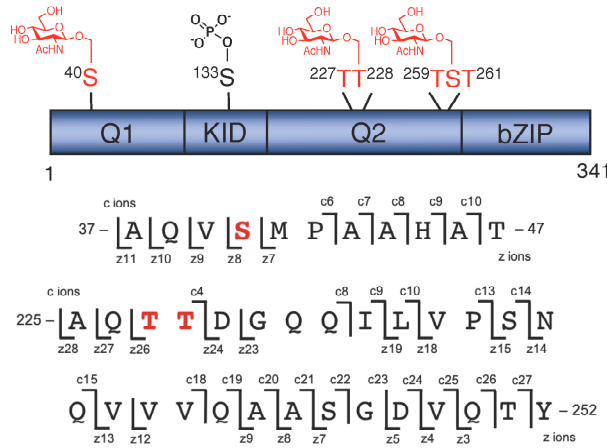


Figure 3: CREB glycosylation sites. Glycosylation sites on CREB mapped by ETD-MS

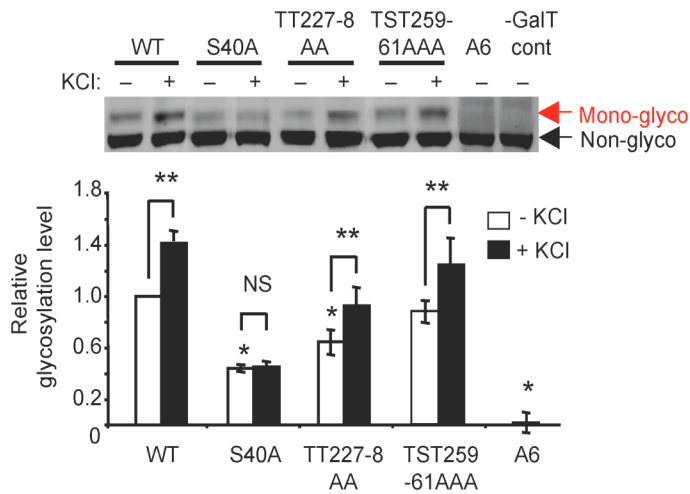


Figure 4: CREB is *O*-GlcNAc glycosylated at Ser40 in response to neuronal activity. Glycosylation levels of Flag-tagged WT CREB and various alanine mutants after expression in cultured cortical neurons. Neurons were depolarized with KCl where indicated. ($n = 7$ for WT and S40A CREB; $n = 3-5$ for other mutants; $*P < 0.01$ compared to WT, unstimulated cells; $**P < 0.05$; NS, not significant). Error bars, means, and standard errors of the mean in this and subsequent figures.

Next, Jessica determined if CREB glycosylation is dynamically modulated by neuronal activity. Membrane depolarization of cortical neurons by treatment with KCl induced glycosylation of CREB. CREB glycosylation levels increased steadily by $42.0 \pm 4.8\%$ over the course of 6 h, in contrast to the rapid induction of CREB phosphorylation at Ser133 (Fig. 5). Mutation of Ser40 to alanine blocked depolarization-induced CREB glycosylation, while mutation of the other glycosylation sites had no effect (Fig. 4). Given the slow kinetics of glycosylation, I examined whether CREB glycosylation is dependent on new protein synthesis. Treatment with the protein synthesis inhibitor

cycloheximide did not block the increase in glycosylation (**Fig. 6**), suggesting that glycosylation is triggered directly by signal transduction pathways. Jessica showed that inhibition of L-type calcium channels with nimodipine abolished the depolarization-induced glycosylation of CREB, indicating a requirement for voltage-sensitive calcium influx (**Fig. 7**). Moreover, inhibition of Ca^{2+} /calmodulin-dependent protein kinases (CaMKs) or mitogen-activated protein kinase (MAPK) blocked the increase in CREB glycosylation, while inhibitors of protein kinase C or protein phosphatases PP-2B or PP-1/2A had no effect (**Fig. 7**). Together, these results show for the first time that neuronal activity stimulates *O*-GlcNAc glycosylation and specifically induces CREB glycosylation at Ser40 in a calcium- and kinase-dependent manner.

CaMKs and MAPK are known to phosphorylate CREB at Ser133, which leads to

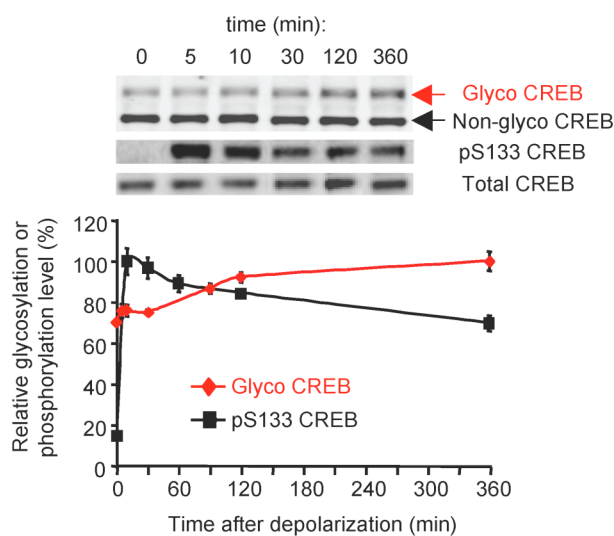


Figure 5: Kinetics of endogenous CREB glycosylation and Ser133 phosphorylation upon depolarization of cortical neurons. Levels of glycosylation or phosphorylation are plotted relative to the maximum signal for each modification. ($n = 4-6$).

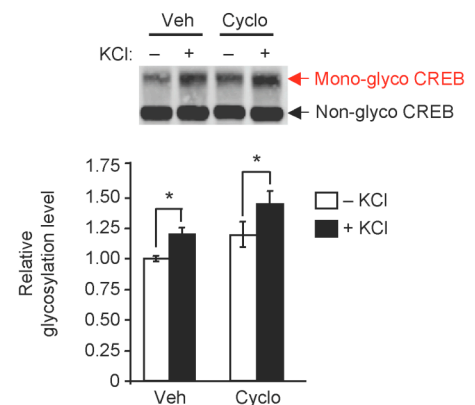


Figure 6: The protein synthesis inhibitor cycloheximide does not block depolarization-induced glycosylation of CREB. Glycosylation levels of endogenous CREB. Neurons were pretreated with cycloheximide (Cyclo) or DMSO vehicle (Veh) and then incubated in the presence or absence of KCl (55 mM) ($n = 3$, $*P < 0.01$).

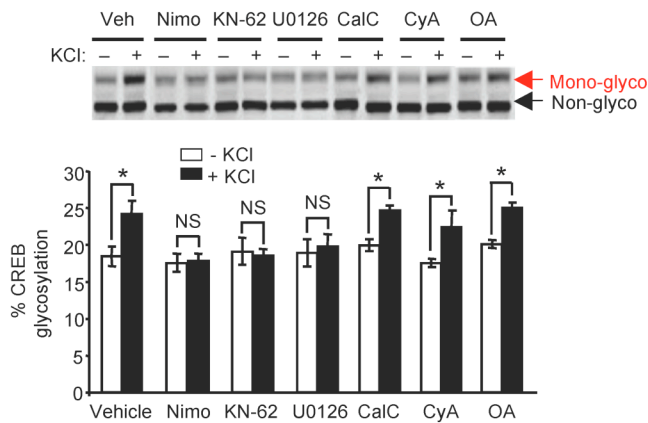


Figure 7: CREB glycosylation is modulated by specific kinase pathways. Glycosylation levels of endogenous CREB in unstimulated or KCl-stimulated cortical neurons upon treatment with inhibitors of L-type calcium channels (nimodipine; nimo), CaMKs (KN-62), MAPK (U0126), protein kinase C (calphostin C; CalC), PP-2B (cyclosporin A; CyA), or PP-1/2A (okadaic acid; OA). ($n = 3-6$, $*P < 0.02$).

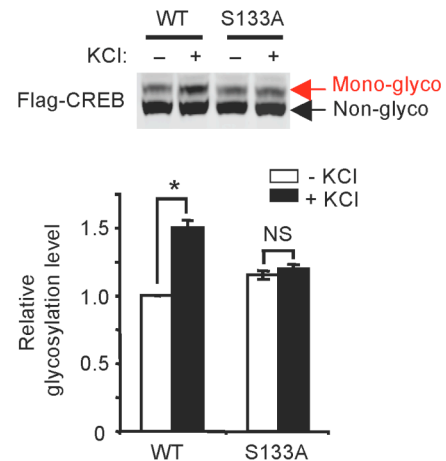


Figure 8: Glycosylation is not induced on S133A CREB. Glycosylation levels were analyzed on Flag-tagged WT or S133A CREB expressed in cortical neurons. ($n = 22$, $*P < 0.001$).

recruitment of the coactivator CREB-binding protein (CBP) and activation of CREB-mediated transcription^{16,17}. As these same kinases are necessary for activity-dependent glycosylation of CREB, Jessica determined whether Ser133 phosphorylation is required for CREB glycosylation. Mutation of Ser133 to Ala (S133A) blocked the KCl-induced increase in CREB glycosylation (**Fig. 8**). However, I showed that forskolin-mediated stimulation of Ser133 phosphorylation via the cAMP pathway failed to induce CREB glycosylation (**Fig. 9**), suggesting that phosphorylation at Ser133 may be required but is not sufficient to activate CREB glycosylation. We recently reported a rapid, chemoenzymatic strategy to probe the interplay between phosphorylation and *O*-GlcNAc glycosylation on target proteins¹⁸. Using this approach, Jessica examined the interdependence of Ser133 phosphorylation and Ser40 glycosylation on CREB. Cortical neuronal lysates were labeled with a 2,000-Da mass tag and immunoblotted with a

phospho-Ser133-specific or total CREB antibody to enable visualization of four distinct subpopulations: (1) mono-glycosylated, (2) nonglycosylated, (3) mono-glycosylated and Ser133-phosphorylated, and (4) nonglycosylated and Ser133-phosphorylated CREB (**Fig. 10**). A significant subpopulation of endogenous CREB was simultaneously phosphorylated and glycosylated in both unstimulated and depolarized neurons (**Fig. 10**), consistent with the notion that phosphorylation and glycosylation cooperatively regulate CREB activity. Moreover, I showed that WT CREB and a mutant form (A5), in which all glycosylation sites except Ser40 were mutated to alanine, showed comparable levels of phospho-Ser133 induction when expressed in neurons, and both Ser40 glycosylation and Ser133 phosphorylation occurred concomitantly on the same protein molecule (**Fig. 11**). Notably, Jessica found that the kinetics of Ser133 phosphorylation upon KCl depolarization was similar for both the glycosylated and nonglycosylated subpopulations of endogenous CREB (**Fig. 10, 12**), indicating that Ser133 phosphorylation occurs independent of the glycosylation state. However, glycosylation was more rapidly induced on the Ser133-phosphorylated subpopulation compared to the total population of endogenous CREB (**Fig. 10, 13**). Collectively, these results strongly suggest that neuronal activity-dependent glycosylation of CREB at Ser40 is induced preferentially on the Ser133-phosphorylated subpopulation.

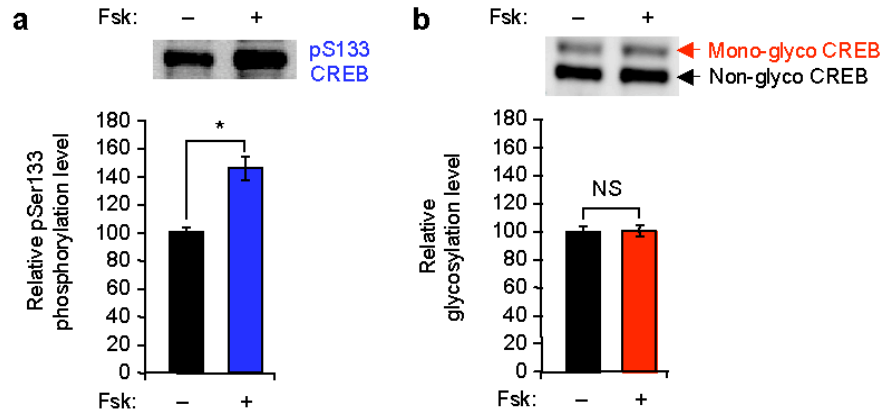


Figure 9: Forskolin induces CREB phosphorylation (a) but not CREB glycosylation (b) in cortical neurons. Neurons were treated with forskolin or DMSO vehicle and lysates were either immunoblotted for pSer133 CREB or chemoenzymatically labeled with a polyethylene glycol mass tag and immunoblotted for CREB to visualize the glycosylated CREB subpopulation. ($n = 3$, $*P < 0.01$; NS, not significant).

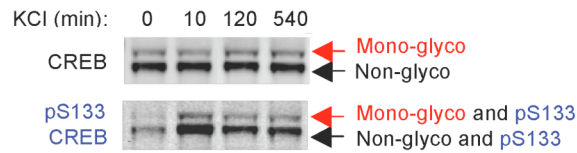


Figure 10: Chemoenzymatic labeling of endogenous CREB for visualizing phosphorylation and glycosylation within the same protein molecule and for quantifying the levels of each modification within distinct post-translationally modified subpopulations

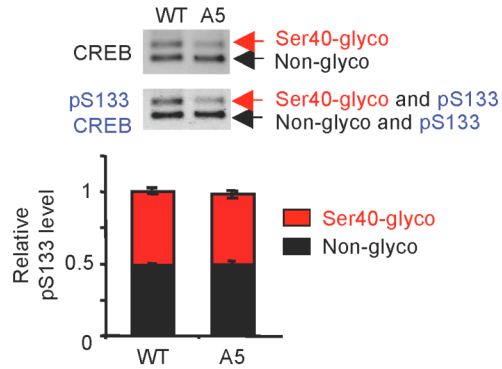


Figure 11: CREB is simultaneously phosphorylated at Ser133 and glycosylated at Ser40. Quantification of pSer133 levels on Flag-tagged WT or A5 mutant CREB following 10-min depolarization. ($n = 3$).

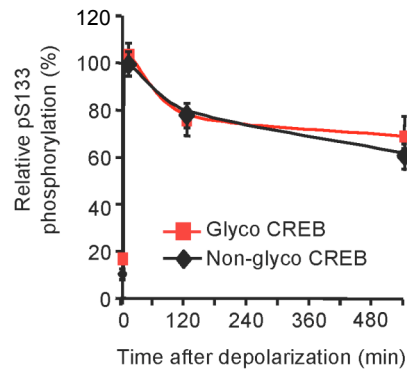


Figure 12: Kinetics of Ser133 phosphorylation for specific post-translationally modified subpopulations of endogenous CREB. ($n = 4$, $*P < 0.03$).

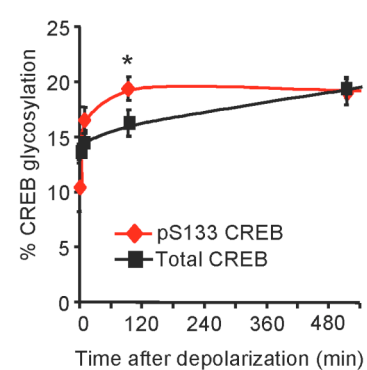


Figure 13: Kinetics of glycosylation for specific post-translationally modified subpopulations of endogenous CREB. ($n = 4$, $*P < 0.03$).

To determine whether glycosylation modulates CREB activity, I compared the ability of wild-type (WT) and S40A mutant CREB to regulate CRE-dependent gene expression. A short hairpin RNA (shRNA) was used to knockdown endogenous CREB in neuro2a neuroblastoma cells, and shRNA-resistant WT or S40A mutant CREB was overexpressed (**Fig. 14**). Replacement of endogenous CREB with the S40A mutant resulted in increased CRE-luciferase activity (**Fig. 15**), suggesting that glycosylation represses the transcriptional activity of CREB. The S40A substitution also upregulated expression of endogenous CREB target genes, including *CDKN1A*, *NR4A2*, and *OPA3*

(**Fig. 16**). To investigate the mechanism, I evaluated whether glycosylation affects the ability of CREB to associate with DNA or transcriptional co-activators. Binding of CREB to the CRE promoter was unaffected by the S40A mutation in an electrophoretic mobility shift assay (**Fig. 17**). However, binding of CREB to CRTC2, a co-activator that stimulates both basal and induced CREB transcription in neurons¹⁹, was significantly enhanced by the S40A mutation in reciprocal co-immunoprecipitation assays (**Fig. 18**).

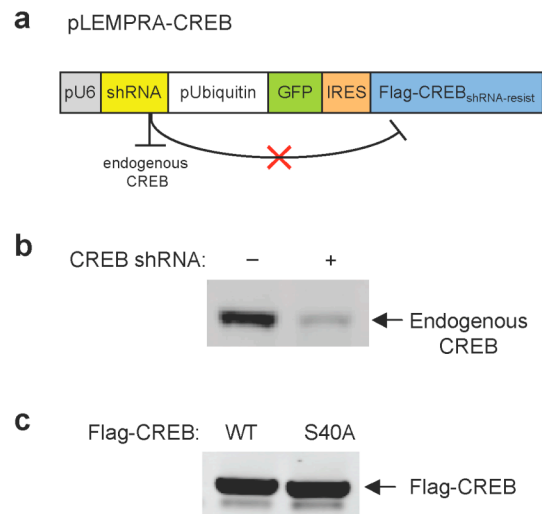


Figure 14: Knockdown of endogenous CREB and overexpression of shRNA-resistant, Flag-tagged WT or S40A CREB in neuro2a cells. **a**, pLEMPRA-CREB construct used to knockdown endogenous CREB and express Flag-tagged CREB. **b**, Knockdown of endogenous CREB using a vector containing the shRNA sequence. **c**, Overexpression of shRNA-resistant CREB from the pLEMPRA construct. Western blots are representative of five independent experiments.

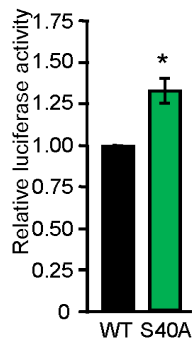


Figure 15: Glycosylation at Ser40 represses CREB activity. CRE-luciferase activity in neuro2a cells expressing WT or S40A CREB. ($n = 11$, $*P < 0.01$).

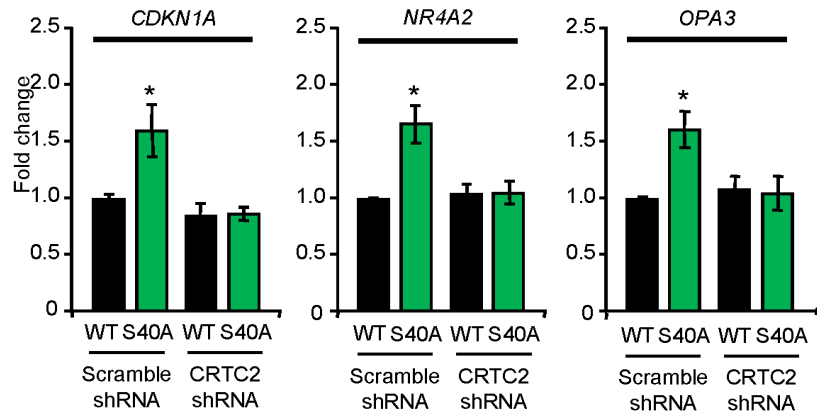


Figure 16: Glycosylation at Ser40 represses CREB activity. Quantitative polymerase chain reaction (qPCR) analysis of *CDKN1A*, *NR4A2*, and *OPA3* expression in cells transfected with the indicated shRNAs or expression vectors using *RPL3* as an internal control ($n = 8$, $*P < 0.01$).

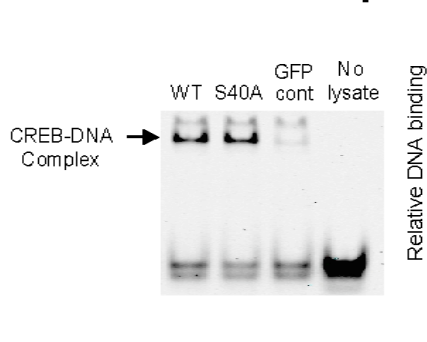


Figure 17: WT and S40A CREB show similar binding to the CRE promoter *in vitro*. Neuro2a cells were transfected with WT or S40A CREB, lysed, and an electrophoretic mobility shift assay was performed using IRDye 700-labeled oligos containing a CRE promoter sequence. ($n = 3$; NS, not significant).

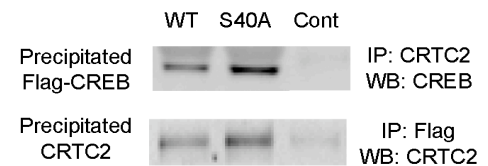


Figure 18: Glycosylation at Ser40 blocks the interaction between CREB and CRTC2. Co-immunoprecipitation of the CREB-CRTC2 complex from neuro2a cells expressing WT or S40A CREB. ($n = 4$).

Furthermore, knockdown of CRTC2 expression in neuro2a cells abolished the observed increases in *CDKN1A*, *NR4A2*, and *OPA3* transcript levels for S40A CREB compared to

WT CREB (**Fig. 16**). Together, these findings indicate that glycosylation impairs the ability of CREB to activate transcription by disrupting the CREB-CRTC interaction.

I next determined whether glycosylation at Ser40 regulates neuronal gene expression, focusing on well-characterized genes involved in brain development and memory consolidation²⁰⁻²⁴. Relative to WT CREB, expression of S40A CREB in cortical neurons increased the levels of *BDNF* exon IV, *Arc*, *Cdk5*, *c-fos*, and *Wnt2* transcripts (**Fig. 19**). Taking into account the contribution of CREB to the expression of each gene, as measured using CREB siRNA, the observed increases correspond approximately to a 2.5–3.6-fold induction in CREB-dependent transcription (**Fig. 20**). Consistent with a mechanism involving direct regulation of these genes through modulation of the CREB-

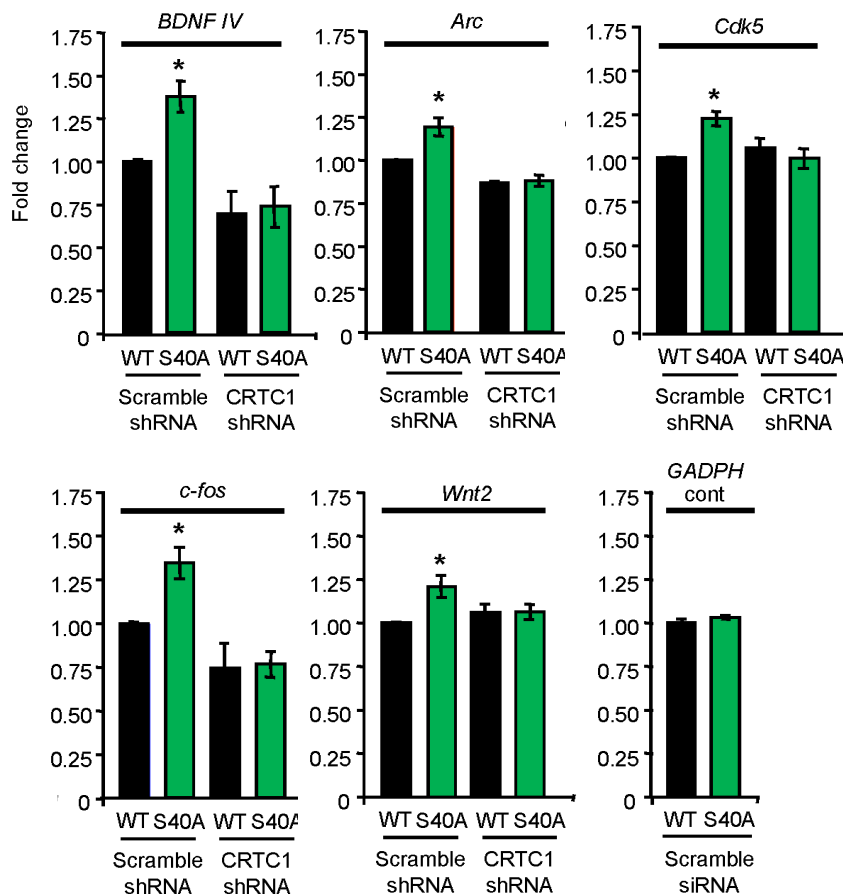


Figure 19: Glycosylation at Ser40 represses CREB activity via a CRTC-dependent mechanism in neurons. qPCR analysis of *BDNF* exon IV, *Arc*, *Cdk5*, *c-fos*, and *Wnt2* expression in cultured cortical neurons electroporated with the indicated siRNAs or expression vectors using *RPL3* as an internal control. ($n = 4-9$, $*P < 0.01$).

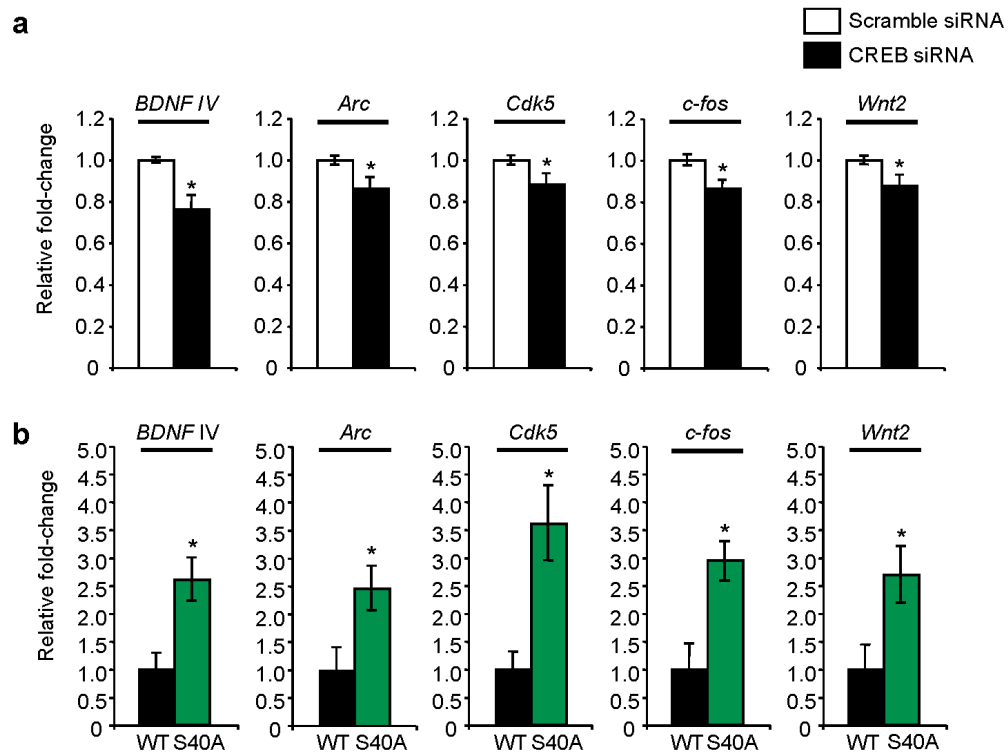


Figure 20: S40A CREB produces approximately a 2.5–3.6-fold increase in mRNA expression relative to WT CREB. **a**, Cortical neurons were electroporated with scramble or CREB siRNA and the mRNA levels of each gene were measured by quantitative RT-PCR. ($n = 14$, $*P < 0.05$). **b**, Cortical neurons were electroporated with WT CREB or S40A CREB and the mRNA levels of each gene were measured by quantitative RT-PCR. The fold-change was calculated by subtracting the transcript level of each gene in neurons transfected with CREB siRNA from the transcript levels of each gene in WT or S40A CREB-expressing neurons and then normalizing the WT CREB levels to 1. ($n = 9$, $*P < 0.01$).

CRTC interaction, both CREB and *O*-GlcNAc transferase (OGT) were bound to the promoters of each gene, and WT and S40A CREB showed comparable levels of promoter occupancy in chromatin immunoprecipitation assays (**Fig. 21, 22**). Moreover, siRNA-mediated knockdown of CRTC1 reversed the effects of S40A CREB on neuronal gene expression (**Fig. 19**). Interestingly, no increases in the transcript levels of *ATF3*, *PEPCK*, or *UCP1* were detected even though CREB was bound to their promoters (**Fig. 23**), suggesting that *O*-glycosylation at Ser40 may confer specificity in the regulation of a subset of CREB-dependent genes. Finally, I investigated the effects of Ser40

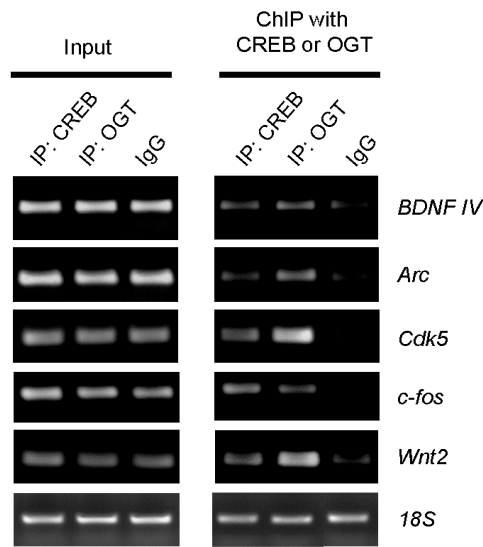


Figure 21: Both CREB and OGT occupy the *BDNF* exon IV, *Arc*, *Cdk5*, *c-fos*, and *Wnt2* promoters. Chromatin immunoprecipitation with an anti-CREB, anti-OGT, or IgG antibody was followed by PCR for the indicated promoters. ($n = 3$).

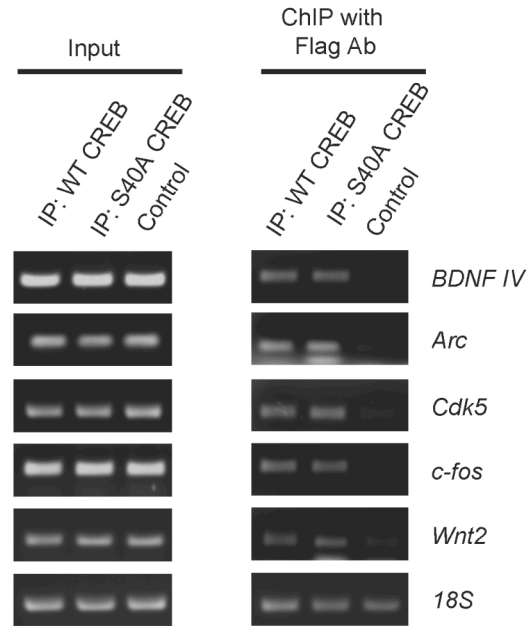


Figure 22: WT and S40A CREB show comparable levels of promoter occupancy on *BDNF* exon IV, *Arc*, *Cdk5*, *c-fos*, and *Wnt2* promoters. Cortical neurons were electroporated with WT or S40A Flag-tagged CREB. Chromatin immunoprecipitation with an anti-FLAG or IgG antibody was followed by PCR for the indicated promoters. ($n = 3$).

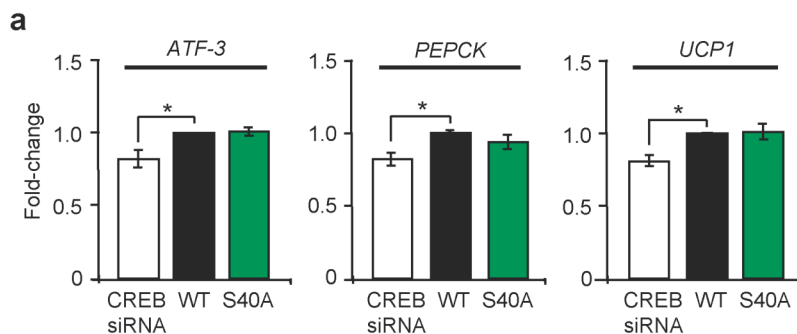


Figure 23: S40A CREB regulates a subset of CREB-mediated genes. **a**, Cortical neurons were electroporated with CREB siRNA, WT CREB, or S40A CREB as noted. Quantitative PCR was performed on the indicated genes. ($n = 4$, $*P < 0.05$). **b**, Chromatin immunoprecipitation was performed with an anti-CREB or IgG control antibody. PCR was carried out using primers specific for the promoters of the indicated genes. Representative gels from three independent experiments are shown.

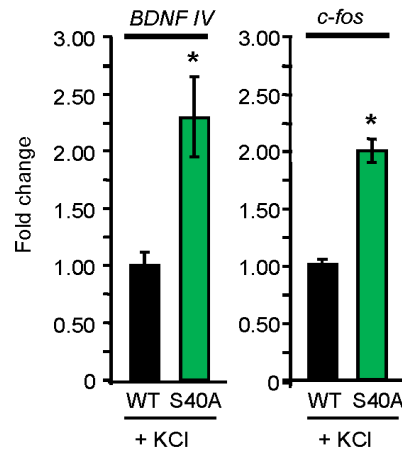


Figure 24: Blocking glycosylation enhances *BDNF IV* and *c-fos* expression even more after depolarization. qPCR analysis of *BDNF* exon IV and *c-fos* expression after membrane depolarization of cultured cortical neurons expressing WT or S40A CREB. ($n = 10$, $*P < 0.01$).

glycosylation on activity-dependent gene expression. Consistent with the observation that neuronal activity enhances CREB glycosylation, blocking glycosylation of CREB at Ser40 increased the levels of *BDNF* exon IV and *c-fos* transcripts to a greater extent in membrane-depolarized neurons compared to unstimulated neurons (Fig. 24). Taken together, the results indicate that CREB glycosylation at Ser40 modulates both basal and activity-dependent gene expression, thereby regulating genes important for neuronal development, survival, and synaptic plasticity.



Figure 25: WT and S40A Flag-tagged CREB are expressed at similar levels in cortical neurons. Cortical neurons were electroporated with WT or S40A CREB. After 3 DIV, the lysate was immunoblotted for Flag-tagged CREB.

CREB has critical roles in several aspects of neuronal development, including axon growth, activity-dependent dendrite development, and synaptogenesis^{10,22,25}. To assess the functional consequences of Ser40 glycosylation on neuronal growth, Jessica assayed axonal and dendritic extension in cortical neurons expressing WT or

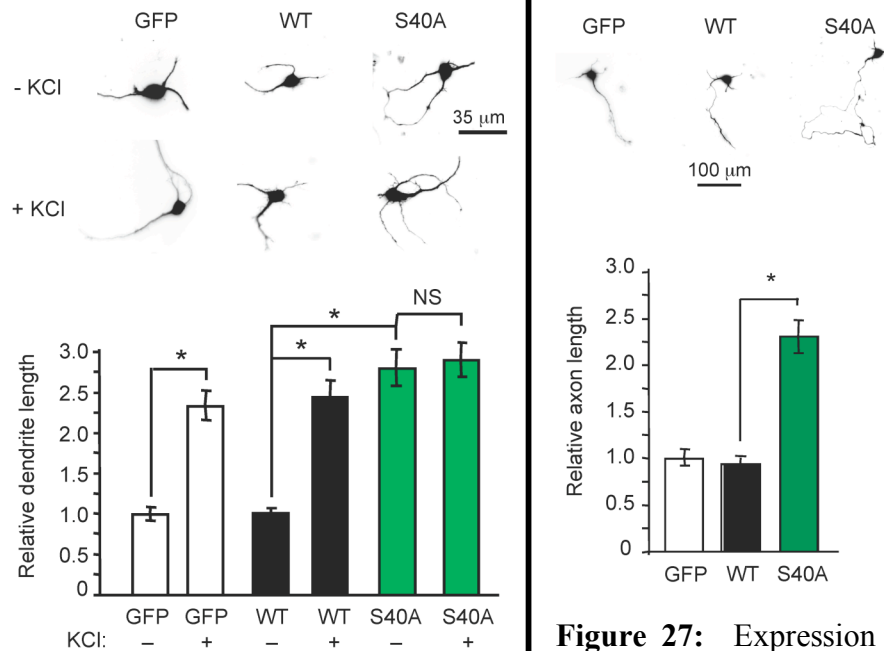


Figure 26: CREB glycosylation at Ser40 represses dendritic growth. Relative total dendrite lengths of cortical neurons expressing GFP, WT CREB or S40A CREB. ($n = 90$ from three independent experiments, $*P < 0.001$; NS, not significant).

Figure 27: Expression of S40A CREB enhances axon outgrowth. Relative axon lengths of cortical neurons expressing, GFP, WT CREB or S40A CREB ($n = 90$ from three independent experiments, $*P < 0.001$).

S40A mutant CREB (**Fig. 25**). Dendrites of neurons expressing WT CREB or a GFP control exhibited similar lengths, and as expected, their growth was stimulated by membrane depolarization (**Fig. 26**). In contrast, neurons expressing S40A CREB had significantly longer dendrites than WT CREB-expressing neurons (2.77-fold increase), displaying lengths comparable to those of depolarized neurons, and their dendrites showed no further elongation upon membrane depolarization (**Fig. 26**). Additionally, neurons expressing S40A CREB had significantly longer axons compared to WT CREB- and GFP-expressing controls (**Fig. 27**). Therefore, preventing CREB glycosylation at Ser40 enhances the outgrowth of both axons and dendrites *in vitro*, indicating that glycosylation has a large, chronic repressive effect on multiple developmental pathways.

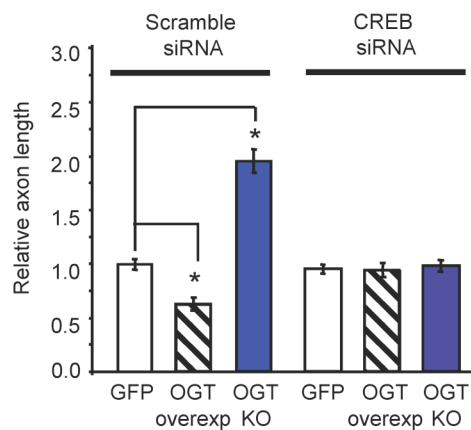
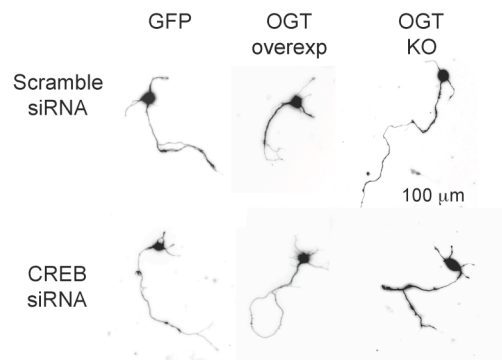


Figure 28: OGT expression represses while OGT knockout enhances axon length. Relative axon lengths of OGT floxed cortical neurons expressing GFP, Flag-tagged OGT, or Cre recombinase (OGT KO). Neurons were also transfected with scramble or CREB siRNA as indicated. ($n = 90$ from three independent experiments, $*P < 0.001$).

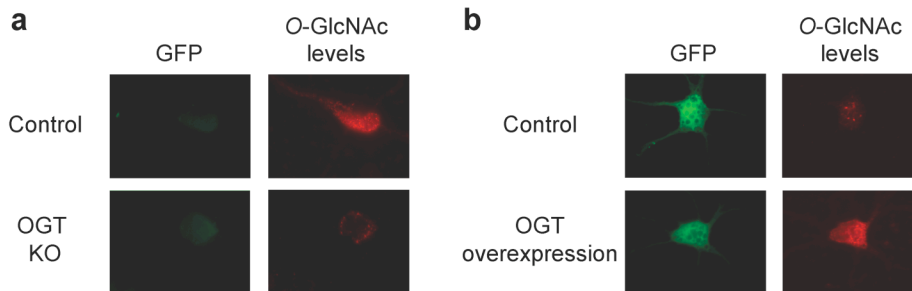


Figure 29: OGT knockout decreases *O*-GlcNAc levels, and OGT overexpression increases *O*-GlcNAc levels. **a**, Neurons from OGT floxed mice electroporated with a GFP construct (control) or with GFP and CRE recombinase constructs (OGT KO). **b**, Neurons from WT mice electroporated with a GFP construct (control) or with an OGT construct containing GFP (OGT overexpression). Cells were immunostained for overall *O*-GlcNAc levels using the pan-specific *O*-GlcNAc antibodies CTD110.6 and RL2, respectively.

To confirm further that these effects are occurring directly through *O*-glycosylation of CREB, Jessica performed OGT gain- and loss-of-function experiments.

OGT-null neurons were generated from OGT floxed mice²⁶ by expression of CRE

recombinase in cultured cortical neurons. Knocking out OGT reduced overall *O*-GlcNAc glycosylation levels and stimulated axonal growth, whereas OGT overexpression enhanced *O*-GlcNAc glycosylation levels and attenuated axonal growth (**Fig. 28, 29**). In both cases, siRNA-mediated knockdown of endogenous CREB reversed the effects of OGT knockout or overexpression and restored axon lengths to those of GFP-expressing neurons (**Fig. 28**), indicating that *O*-GlcNAc glycosylation modulates axonal growth through a CREB-dependent mechanism.

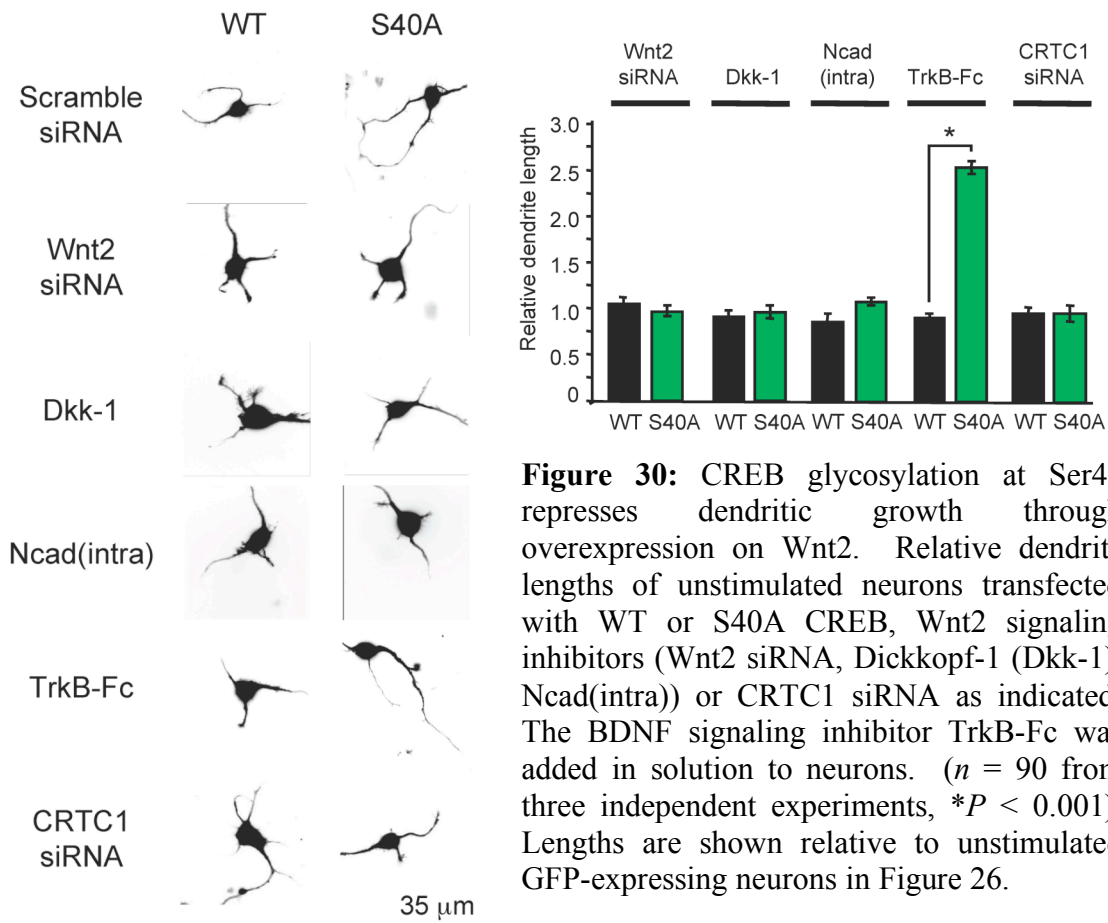


Figure 30: CREB glycosylation at Ser40 represses dendritic growth through overexpression on Wnt2. Relative dendrite lengths of unstimulated neurons transfected with WT or S40A CREB, Wnt2 signaling inhibitors (Wnt2 siRNA, Dickkopf-1 (Dkk-1), Ncad(intra)) or CRTCl siRNA as indicated. The BDNF signaling inhibitor TrkB-Fc was added in solution to neurons. ($n = 90$ from three independent experiments, $*P < 0.001$). Lengths are shown relative to unstimulated GFP-expressing neurons in Figure 26.

To investigate the molecular mechanisms further, Jessica and I considered known mediators of CREB-dependent dendrite and axon elongation. Activation of CREB drives the expression of the secreted mitogen *Wnt2* to regulate activity-dependent dendritic growth, whereas application of the neurotrophin BDNF leads to axon elongation^{22,27}. Both *Wnt2* and *BDNF* transcript levels were significantly increased in cortical neurons expressing S40A CREB as compared to WT CREB (**Fig. 19**). I showed that knockdown of *Wnt2*, overexpression of the *Wnt2* antagonist Dickkopf-1, or overexpression of the β -catenin sequestrant *Ncad*(intra) reversed the stimulatory effects of both S40A CREB (**Fig. 30**) and neuronal depolarization (**Fig. 31**) on dendritic growth. Alternatively, Jessica showed that treatment with the BDNF/NT-4/5 scavenger TrkB-Fc blocked the effects of S40A CREB specifically on axon growth, but not dendrite growth (**Fig. 30, 32**). Moreover, knockdown of *CRTC1* abolished the S40A CREB-dependent increases in *Wnt2/BDNF* gene expression (**Fig. 19**), dendritic growth (**Fig. 30**), and axonal growth

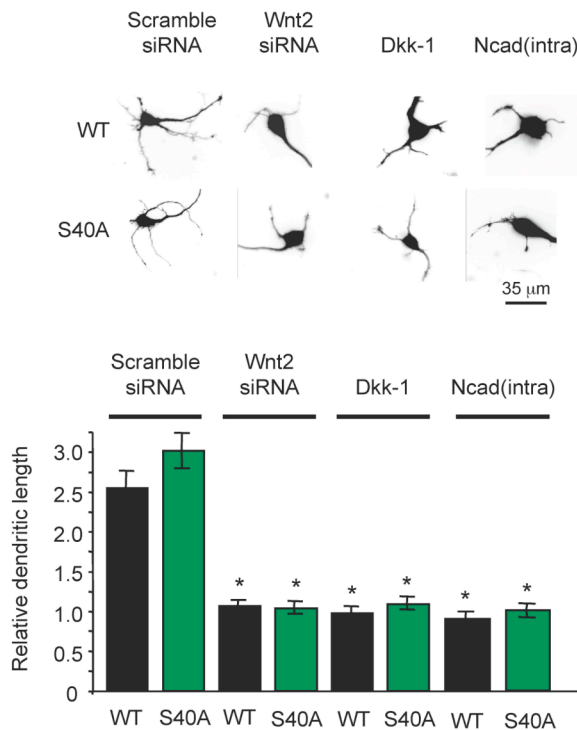


Figure 31: Depolarization-induced dendrite growth is blocked by *Wnt2* siRNA, *Dkk-1*, and *Ncad*(intra). Relative axon lengths of cortical neurons were electroporated with Flag-tagged WT or S40A CREB constructs containing GFP, along with scramble siRNA, *Wnt2* siRNA, *Dkk-1*, or *Ncad*(intra) constructs and treated with KCl as indicated. Lengths relative to neurons expressing WT CREB in the absence of KCl stimulation are shown. (* $P < 0.001$ relative to scramble siRNA for each respective genotype).

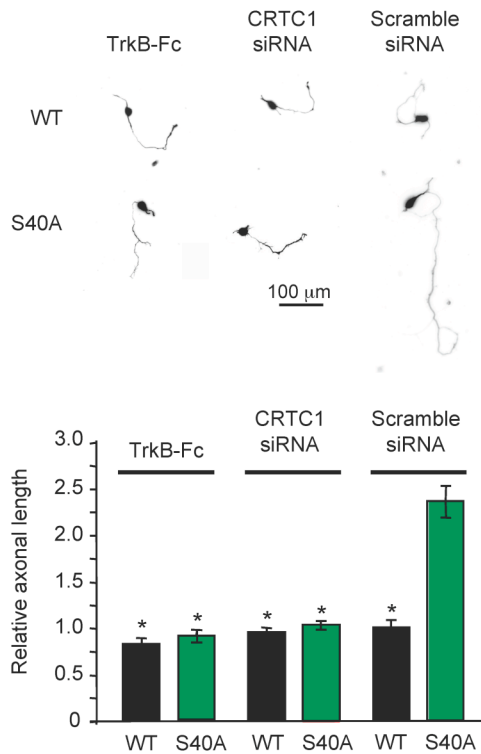


Figure 32: The enhanced axon outgrowth caused by expression of S40A CREB is blocked by TrkB-Fc or CRTC1 knockdown. Cortical neurons were electroporated with Flag-tagged WT or S40A CREB constructs containing GFP, along with CRTC1 or scramble siRNA as indicated. TrkB-Fc (0.7 $\mu\text{g/ml}$) or vehicle was added after 1 DIV where indicated. ($n = 90$ from three independent experiments, $*P < 0.0001$).

(**Fig. 32**). Thus, CREB glycosylation modulates dendrite and axon elongation via the CRTC-dependent downregulation of Wnt2 and BDNF signaling, respectively. These findings strongly suggest that *O*-glycosylation of CREB functions as a critical regulator of neuronal growth. By controlling the basal threshold levels of key genes, glycosylation of CREB exerts a chronic repressive effect on neuronal growth and enables appropriate stimuli-induced growth responses.

Having shown that *O*-GlcNAc glycosylation modulates important CREB-dependent cellular processes, we next examined the role of CREB glycosylation in higher-order brain functions *in vivo*. CREB-dependent transcription is essential for the consolidation of long-term conditioned fear memories^{14,28}. Jessica and I first examined whether glycosylation is induced on endogenous CREB in response to auditory fear conditioning. Specifically, the glycosylation levels of CREB were compared in the lateral amygdala of fear-conditioned mice and tone-only trained controls. An increase in glycosylation ($13.6 \pm 0.3\%$) was detected specifically within the activated CREB subpopulation (phosphorylated at Ser133; **Fig. 33**), indicating that glycosylation

of CREB is induced following activation of amygdala neurons *in vivo*. To determine whether CREB glycosylation affects memory formation *in vivo*, Jessica bilaterally microinjected replication-defective herpes simplex viral (HSV) vectors expressing WT CREB and GFP, S40A CREB and GFP, or GFP alone into the lateral amygdala of mice before fear conditioning (**Fig. 34**), and assessed memory 30 min, 2 h, and 24 h after training. Similar to previous experiments^{29,30}, mice infused with WT CREB vector had enhanced memory compared to GFP vector-infused mice after 24 h, but not after 30 min or 2 h (**Fig. 35**; $F_{1,25} = 4.34$, $P = 0.048$), indicating that CREB overexpression increases long-term fear memory. Notably, Jessica found that mice infused with S40A CREB vector exhibited significant memory enhancement 2 h after training compared to mice infused with WT CREB or GFP (**Fig. 35**; $F_{2,45} = 9.70$, $P = 0.0003$). To test whether this effect represents enhanced long-term memory, a CREB-dependent process that requires *de novo* mRNA and protein synthesis^{14,28}, Jessica injected the mice with the protein synthesis inhibitor, anisomycin, at various points after training and then assessed memory. Inhibiting protein synthesis immediately after training blocked the memory enhancement of S40A CREB at 2 h (**Fig. 36**; $F_{1,12} = 24.57$, $P = 0.0003$), while inhibiting protein synthesis 2 h after training failed to block the memory enhancement at 24 h (**Fig. 37**; $F_{1,13} = 0.23$, $P = 0.64$). These results indicate that mice expressing S40A CREB have enhanced, consolidated long-term memory at 2 h. As with the neurite outgrowth studies, we observed an accelerated response upon removing the repressive effects of glycosylation. Limited information is known about the genes and mechanisms that control the rate of memory consolidation. However, our results are consistent with the requirement for *de novo* gene expression and suggest that blocking CREB glycosylation

leads to the accumulation of plasticity-related transcripts and the facilitation of rapid long-term memory consolidation. More broadly, these findings provide the first direct demonstration that *O*-GlcNAc glycosylation plays a role in higher-order brain functions.

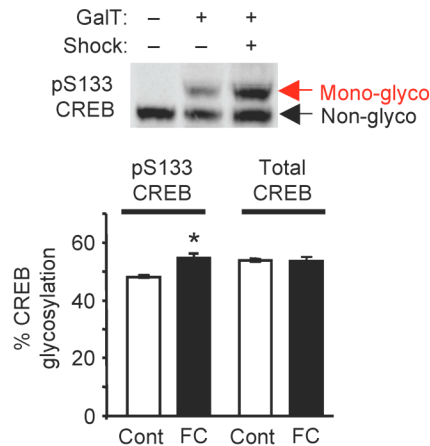


Figure 33: CREB glycosylation is induced following activation of neurons *in vivo*. Glycosylation levels of activated Ser133-phosphorylated CREB and total CREB in the amygdala 15 min after auditory fear conditioning. ($n = 3$, $*P < 0.01$).

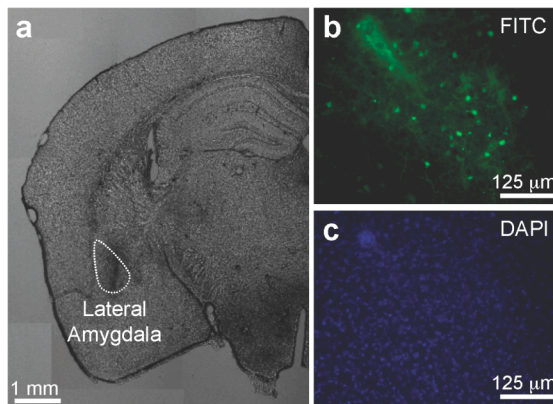


Figure 34: Herpes simplex virus (HSV) infection of the lateral amygdala of mice. The lateral amygdala [AP = -1.3, ML = +/-3.3, V = -4.8 from bregma] of 9–10 week old male C57BL/6 mice was injected with WT CREB, S40A CREB, or GFP HSV (1.5 ml) for 25 min. **a**, Bright field image of a representative brain section infused with WT CREB vector showing an outline of the lateral amygdala. **b**, FITC image of injection site. **c**, DAPI image of (b)

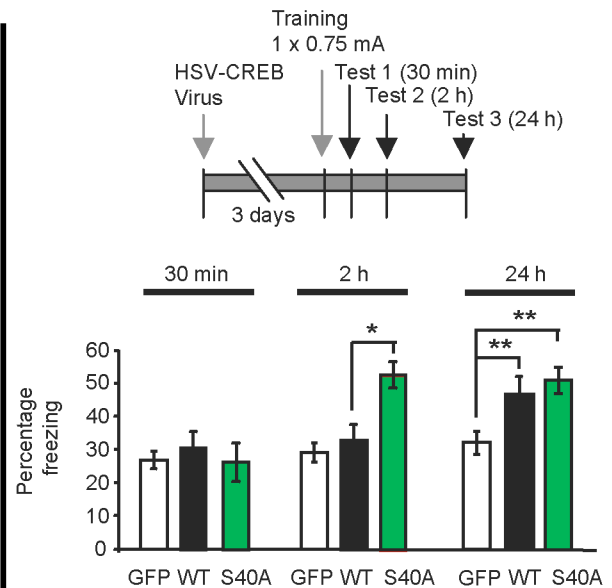


Figure 35: CREB glycosylation at Ser40 modulates long-term conditioned fear memory. Freezing behavior after auditory fear conditioning of mice infused with HSV vectors expressing GFP, WT or S40A CREB. ($n = 11$ for GFP, $n = 16$ for WT, and $n = 20$ for S40A at 2 h and 24 h, $n = 6$ for all vectors at 30 min. $*P < 0.05$ compared to GFP after 24 h, $**P < 0.0005$ compared to WT and GFP at 2 h).

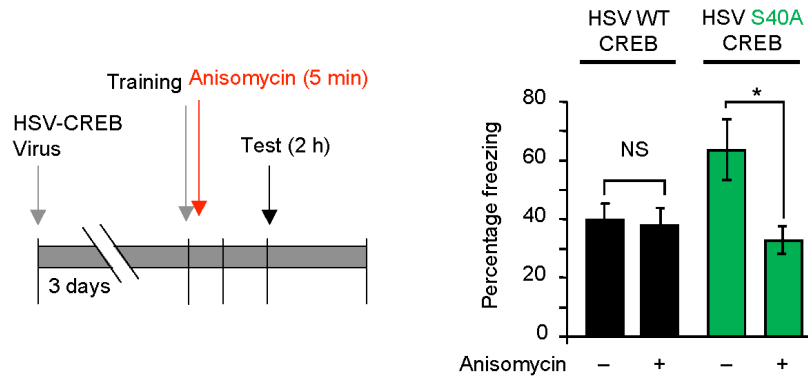


Figure 36: Inhibition of protein synthesis immediately after training blocks the memory enhancement of S40A CREB at 2 h. Replication-defective HSV vectors expressing WT CREB and GFP, S40A CREB and GFP, or GFP alone were bilaterally microinjected into the lateral amygdala of mice 3 days prior to auditory fear conditioning training. Mice were injected with anisomycin or saline 5 min after fear conditioning, and freezing behavior was assessed after 2 h. ($n = 6$ for WT, $n = 7$ for S40A, $*P < 0.0005$; NS, not significant)

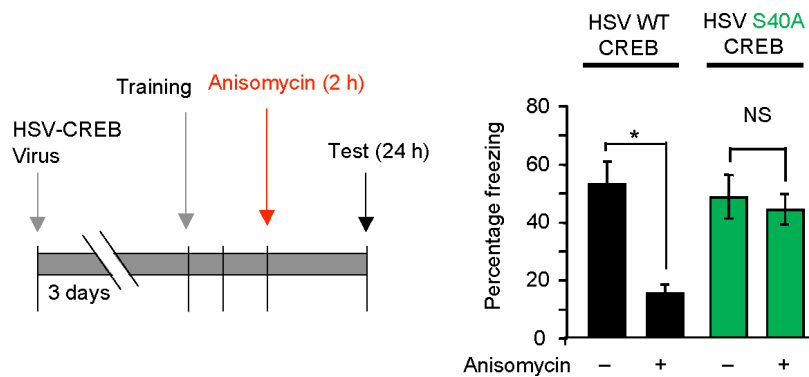


Figure 37: Inhibition of protein synthesis 2 h after training blocks the memory enhancement of WT CREB at 24 h, but not that of S40A CREB. Replication-defective HSV vectors expressing WT CREB and GFP, S40A CREB and GFP, or GFP alone were bilaterally microinjected into the lateral amygdala of mice 3 days prior to auditory fear conditioning training. Mice were injected with anisomycin or saline 2 h after fear conditioning, and freezing behavior was assessed after 24 h. The memory enhancement of S40A CREB at 24 h was anisomycin-resistant. ($n = 6$ for WT, $n = 8$ for S40A anisomycin, $n = 7$ for S40A saline, $*P < 0.005$; NS, not significant).

The importance of dynamic *O*-GlcNAc glycosylation in the regulation of glucose homeostasis and insulin signaling is well appreciated^{1,3-5}. Our study expands the scope of

cellular regulation by *O*-glycosylation to the brain and demonstrates that it serves functions in the brain comparable to other major posttranslational modifications such as phosphorylation. We show that *O*-glycosylation is dynamically modulated by neuronal signaling pathways and works cooperatively with Ser133 phosphorylation to allow for graded suppression of the activated CREB subpopulation. *O*-Glycosylation also suppresses the constitutive transcriptional activity of CREB in quiescent neurons and limits basal gene expression levels, allowing for a larger dynamic range of induction and proper activity-induced responses such as neuronal growth and memory consolidation. In these ways, glycosylation enables the fine-tuned, exquisite coupling of extracellular stimuli to transcriptional regulation in ways not achieved by phosphorylation or transcriptional repressors. Collectively, our results demonstrate how site-specific protein *O*-glycosylation contributes to complex neuronal processes and reveal its potential as a critical regulator of higher-order brain function.

Methods

Construction of expression plasmids and viruses. All constructs were generated using standard molecular biology methods and verified by DNA sequencing.

pLEMPRA CREB. Rat CREB cDNA, containing an N-terminal Flag tag, was cloned into the lentiviral expression vector pLEMPRA-GOI (provided by M. Greenberg) immediately following the GFP-IRES sequence. Subsequently a CREB shRNA cassette (described below) was subcloned into the pLEMPRA vector. The CREB sequence was made shRNA-resistant by introducing the following five silent mutations (lower case

letters): GGAGagcGTGGATAGcGTg. Various CREB alanine mutations were created from the resulting vector using the QuikChange Lightning Mutagenesis kit (Stratagene).

pLenti CREB. The pLenti WT and alanine mutant CREB plasmids were created by subcloning Flag-tagged WT and alanine mutant CREB sequences from the pLEMPRA CREB vectors in place of the H2B sequence in the lentiviral expression plasmid pLenti PGK:H2B:mCherry (provided by R. Lansford). A T2A sequence was inserted between the CREB and mCherry sequences.

shRNA. shRNA sequences targeting mouse CREB (5'-GGAGTCTGTGGATAGTGTA-3'³¹), mouse CRT2 (5'-GATGCTAAAGTCCCTGCTATT-3') or no mouse transcript (5'-CAACAAGATGAAGAGCACC-3'; scramble) were inserted into the lentiviral expression vector pLLX-shRNA³².

HSV CREB. The S40A HSV CREB plasmid was constructed by cloning S40A rat CREB cDNA in place of WT CREB into the bicistronic HSV amplicon p1005+:CREB (provided by S. Josselyn), in which CREB and eGFP expression are driven by IE4/5 and T7 promoters, respectively. The amplicons were packaged as previously described³⁰.

pA2UCOE-OGT. Rat OGT cDNA was first cloned into the pLEMPRA-GOI vector immediately following the GFP-IRES-Flag sequence. Subsequently the entire GFP-IRES-Flag-OGT sequence was subcloned in place of the EGFP sequence in the lentiviral expression vector pA2UCOE-EGFP³³.

Cell cultures and transfection. Neuro2a cells were maintained in DMEM supplemented with 10% fetal bovine serum (FBS) and penicillin/streptomycin (100 U ml⁻¹). Transfections were performed using Lipofectamine LTX and PLUS reagents according to the manufacturer's protocol (Invitrogen).

Cortical neuronal cultures were prepared as previously described¹⁸, except that neurons from E15-16 timed-pregnant C57BL/6 mice were plated onto poly-DL-lysine coated plates or coverslips. For pharmacological treatment and ChIP experiments, neurons were cultured in Neurobasal medium (NBM) supplemented with 2 mM Glutamax-I, penicillin/streptomycin (100 U ml⁻¹), and 2% B-27 (Invitrogen). For reverse transcription PCR (RT-PCR) and neurite outgrowth experiments, neurons were cultured in NBM supplemented with 10% FBS and 2 mM Glutamax-I. Neurons were electroporated with vectors and siRNA using the program K-09 on the Nucleofector Device (Lonza) according to the manufacturer's instructions.

Quantification of *O*-GlcNAc glycosylation and Ser133 phosphorylation levels on CREB. For those experiments using exogenously expressed CREB mutants (**Figs. 4, 8, 11**), WT or mutant pLenti CREB constructs were electroporated into neurons. Neurons were treated with the following after 4-6 DIV: KCl (55 mM, 2 h for **Figs. 4, 6, 7, 8**; 10 min for **Fig. 11**; 10 min–9 h for **Figs. 5, 10, 12, 13**), forskolin (10 μM, 2 h). Prior to KCl treatments, both treated and control neurons were silenced overnight with tetrodotoxin (TTX, 1 μM; Tocris Biosciences). Where indicated, cells were treated with the following

inhibitors for 30 min prior to the addition of KCl: nimodipine (5 μ M), KN-62 (5 μ M), U0126 (10 μ M), calphostin C (2.5 μ M), cyclosporin A (5 μ M), okadaic acid (50 nM), cycloheximide (0.3 mg ml⁻¹) or vehicle (water, EtOH, or DMSO). All drugs except KCl and TTX were from Axxora Alexis.

Cultured neurons or dissected brain tissues were lysed and chemoenzymatically labeled with a PEG mass tag as previously described¹⁸. The lysates were subjected to 4–12% SDS-PAGE (Invitrogen) and immunoblotted. Anti-CREB (Chemicon) and anti-phospho-Ser133 CREB (Affinity BioReagents) antibodies were used to quantify the percentage of glycosylation on endogenous CREB (**Figs. 1, 5, 6, 7, 9, 10, 12, 13**). An anti-Flag (Sigma) antibody was used to quantify the percentage of glycosylation on exogenously expressed CREB mutants (**Figs. 4, 8, 11**). Relative levels of S133 phosphorylation were measured by normalizing phospho-Ser133 levels to total CREB levels. Western blots were visualized and quantified using an Odyssey Infrared Imaging System and software (Li-Cor, Version 2.1).

Identification of *O*-GlcNAc glycosylation sites on CREB. Neuro2a cells transfected with WT pLEMPRA CREB were treated with *O*-(2-acetamido-2-deoxy-D-glucopyranosylidene)amino *N*-phenylcarbamate (PUGNAc, 100 μ M, 6 h; Toronto Research Chemicals) to inhibit β -*N*-acetylglucosaminidase and lysed in 1.5% SDS-containing protease inhibitor cocktail (PIC; Roche) and 5 μ M PUGNAc. The lysate (7.5 mg) was diluted 1.5-fold, quenched with one volume of NETFS buffer (100 mM NaCl, 50 mM Tris-HCl pH 7.4, 5 mM EDTA, PIC, 5 μ M PUGNAc) containing 6% (v/v) NP-

40 and then was further diluted to 2 mg ml⁻¹ with NETFS buffer. The sample was passed over 400 µl of anti-Flag M2 affinity gel three times, washed three times with 10 ml of NETFS containing 1% (v/v) NP-40, washed twice with 10 ml of NETFS, eluted in 400 µl of 4% SDS, 100 mM Tris pH 7.9, and concentrated to a volume of 20 µl. After SDS-PAGE (4–12% Bis-Tris gels), the CREB band was excised and manually digested in-gel with chymotrypsin as previously described³⁴. Nano LC-MS of peptides was performed as previously described using a 60-min linear gradient on an LTQ XL (Thermo Fisher)³⁵. MS/MS spectra were collected in both CID and ETD modes using separate analyses. MS/MS were searched using Mascot 2.2 against a custom database containing Flag-CREB and 200 other proteins. ETD spectra were first converted to *.DTA files using RawXtract (Version 1.9.1) and allowing charge states up to +5 prior to conversion to the MGF file format using Bioworks (Version 3.3.1). Searches were performed with an enzyme specificity of chymotrypsin at one terminus only, fixed modification of carbamidomethyl (C), and variable modifications of oxidation (M) and GlcNAc (S,T). The search results were evaluated by applying a Mascot Ion Cutoff score of 20 and then manually evaluating each putative GlcNAc modified peptide. Raw CID data was further evaluated for the prominent neutral loss of GlcNAc using SALSA³⁵.

Luciferase reporter assays. Neuro2a cells were transfected with WT or S40A pLEMPRA CREB, pCRE-Luc (Stratagene), pRL-TK (Promega), and CREB shRNA vectors as indicated. The cells were cultured for 72 h, and luciferase activities were measured with the Dual-Glo Luciferase Assay System (Promega) on a Victor 3 plate reader (Perkin Elmer). pRL-TK containing *Renilla* luciferase was used to normalize for

transfection efficiency. Lysates from neuro2a cells transfected with CREB or scramble shRNA, and WT or S40A pLEMPRA CREB were immunoblotted for CREB to confirm endogenous CREB knockdown and equal levels of WT and S40A CREB expression.

Electrophoretic mobility shift assay (EMSA). Neuro2a cells were transfected with WT or S40A pLEMPRA CREB and CREB shRNA vectors or the pMaxGFP (Lonza) control vector alone. The nuclear fractions were isolated³⁶, and the DNA-binding reaction was performed for 30 min at room temperature in the dark. The 20- μ l reaction consisted of protein (5 μ g), 10 mM Tris pH 7.5, 150 mM KCl, 10 mM DTT, 0.25 mM EDTA, Poly(dIdC) (2 μ g; Pierce), 20 μ M PUGNAc, 2% glycerol, and IRDye 700-labeled EMSA oligos containing a CRE sequence (1 μ l; Li-COR). The samples were resolved on a 10% polyacrylamide gel, and bands were quantified using an Odyssey Infrared Imaging System.

Co-immunoprecipitation of the CREB-CRTC complex. Neuro2a cells were transfected with WT or S40A pLEMPRA CREB and CREB shRNA vectors. After 72 h, the cells were lysed in 25 mM Tris pH 7.8, 1 mM EDTA, 150 mM NaCl, 0.5% NP-40, 5 μ M PUGNAc, and protease inhibitors. After pre-clearing the lysate with protein A sepharose beads (GE Healthcare), the lysates were immunoprecipitated with anti-Flag M2 affinity gel or an anti-CRTC2 antibody (Calbiochem). The co-immunoprecipitated complexes were resolved by 4–12% SDS-PAGE and immunoblotted for Flag-CREB and CRTC2. For the Flag IP control, nontransfected samples were immunoprecipitated with

anti-Flag M2 affinity gel. For the CRTC2 IP control, transfected samples were immunoprecipitated with a rabbit IgG antibody (Santa Cruz).

Quantitative RT-PCR (qPCR). For neuro2a gene expression experiments, the cells were transfected with WT or S40A pLEMPRA CREB, CREB shRNA, and scramble or CRTC2 shRNA. For neuronal gene expression experiments, cortical neurons were electroporated with WT or S40A pLEMPRA CREB and scramble (UUCUCCGAACGUGUCACGUdTdT) or CRTC1 (CGAACAAUCCGCGGAAAUdTdT) siRNA³⁷. To measure the contribution of CREB to the expression of each gene, neurons were electroporated with scramble or CREB siRNA (UACACUAUCCACAGACUCCdTdT)³¹. After 3–4 days, neurons were pretreated overnight with TTX and depolarized with KCl for 6 h (where indicated), and the mRNA was extracted and purified using an RNeasy kit (Qiagen) and reverse-transcribed with SuperScript III and random primers (Invitrogen) according to the manufacturer's protocol. Quantitative PCR was performed with FastStart Universal SYBR Green Master (Rox; Roche) using an ABI 7300 real-time instrument, version 1.2. Relative quantities of mRNA were normalized to the ribosomal protein L3 (RPL3) mRNA content. PCR primers are described in **Table 1**.

Chromatin Immunoprecipitation (ChIP). For experiments with exogenously expressed CREB mutants (**Fig. 23**), WT or S40A pLenti CREB constructs were electroporated into neurons. ChIP was performed as previously described³⁸, except that the neurons were fixed for 20 min, the samples were treated with proteinase K (10 mg

ml⁻¹) for 2 h at 37 °C after elution, and the DNA was isolated by phenol/chloroform extraction followed by ethanol precipitation. Samples were immunoprecipitated using protein A sepharose beads and anti-OGT (provided by G. Hart), anti-CREB (Upstate), anti-Flag M2, and anti-rabbit IgG (Santa Cruz) antibodies. In the case of the Flag IP, a control IP of nontransfected lysate with anti-Flag antibody was performed. Purified DNA samples were subjected to PCR for 36 cycles. PCR primers are described in Table 2.

Table 1. Primers used for RT-PCR

Gene name	Forward primer 5' – 3'	Reverse primer 5' – 3'
<i>Arc</i>	TGGAGCAGCTTATCCAGAGG	TATTCAGGCTGGGTCTCTGTC
<i>ATF3</i>	CCAAGAGCCGTTGGGGCAGG	TCACTCGGGGGCAGAGTGGG
<i>BDNF IV</i>	CAGAGCAGCTGCCTTGATGTT	GCCTTGCCGTGGACGTTTA
<i>Cdk5</i>	TTTCCCTCCCTCCGTG	TGGGAAAGGAGCCAATTTATG
<i>CDKN1A</i>	GTTCCGCACAGGAGCAAAG	GAGTGCAAGACAGCGACAAG
<i>c-fos</i>	CCGACTCCTTCTCCAGCAT	TCACCGTGGGGATAAAGTTG
<i>GADPH</i>	CTGAGTATGTCGTGGAGTCTACTGG	GTCATATTTCTCGTGGTTCACACC
<i>NR4A2</i>	GCATACAGGTCCAACCCAGT	AATGCAGGAGAAGGCAGAAA
<i>OPA3</i>	GCAAAGGCAAAAGATGGAAC	GTGTTCAACCAAGGAAGGAG
<i>PEPCK</i>	GGGCCTGCAACCCTGAGCTG	GGCGATCCGCAACGCAAAGC
<i>RPL3</i>	TCATTGACACCACCTCCAAA	GCACAAAGTGGTCCTGGAAT
<i>UCP1</i>	TTGAGCTGCTCCACAGCGCC	CCGCGACTTCGGACTCCTGC
<i>Wnt2</i>	CATAGCCCCCACCCTGT	AGTTCCTTCGCTATGTGATGTTTCT

Table 2. Primers used for ChIP PCR

Gene name	Forward primer 5' – 3'	Reverse primer 5' – 3'
<i>Arc</i>	GGCTGGCTCTGGGAGGTATTTA	CCCCCAGAGCTGAGAGTTCAGA
<i>ATF3</i>	CCAGTTCTCCCTGGAAGCTA	CGTTGCATCACCCCTTTTAA
<i>BDNF exon IV</i>	TGGACTCCCACCCACTTT	GTGGCCGATATGTACTCC
<i>Cdk5</i>	GCTGAAGCTGTCAGGAGGTC	GTGCCCCGCTCTTGTATTATA
<i>c-fos</i>	CCTCCCTCCTTTACACAG	GTCTTGGCATAACATCTTTC
<i>PEPCK</i>	GGCCTCCCAACATTCATTAAC	GTAGCCCCGCCCTCCTTGCTTTAA
<i>UCP1</i>	TCCTCTGGGCATAATCAGGAACT	CAGGTCTCAAAGAGCTGCTAGT
<i>Wnt2</i>	CCCGCACACGGAGTCTGACC	AATCCATCAGCACCGCGCCC
<i>18S Ribosomal RNA</i>	CGCGTTCTATTTTGTGGT	AGTCGGCATCGTTATGGTC

Neurite Outgrowth. Neurons were electroporated with WT or S40A pLEMPRA, pMaxGFP, pcDNA3-Dkk-1-Flag (provided by X. Yu), or Ncad(intra) (provided by X. Yu) vectors and scramble, CRTCl, or Wnt-2 siRNA (Santa Cruz) as indicated and then plated at a density of 25,000 neurons cm^{-2} . Neurons from B6.129-*Ogt*^{tm1Gwh}/J mice (Jackson Laboratories) were electroporated with pMaxGFP, the CRE recombinase pBOB-CAG-iCRE-SD (Addgene), or pA2UCOE-OGT vector, along with scramble or CREB siRNA as indicated. One day prior to imaging for dendrites, neurons were depolarized with KCl (50 mM) where indicated. After 1 DIV, neurons were treated with TrkB-Fc (R&D Biosystems; 0.7 $\mu\text{g ml}^{-1}$) where indicated. After 4–5 DIV, all neurons were fixed with 4% paraformaldehyde (PFA) for 20 min at room temperature, washed twice with PBS, once with H₂O, and mounted onto glass slides. Transfected GFP-expressing cells were imaged using a Nikon Eclipse TE2000-S inverted microscope equipped with Metamorph software. Neurite lengths were quantified with NeuronStudio (Version 0.9.92)³⁹. Lysates from neurons electroporated with WT or S40A CREB were immunoblotted for Flag-CREB to confirm equal levels of CREB expression. Neurons from B6.129-*Ogt*^{tm1Gwh}/J or C57BL/6 mice were immunostained with an anti-OGT (Sigma) or anti-*O*-GlcNAc antibody (CTD110.6, Covance or RL2, Pierce) to confirm the effects of OGT knockdown and overexpression on OGT and *O*-GlcNAc levels, respectively.

Auditory fear conditioning. *Surgery:* 9–10 week old male C57BL/6 mice (Charles River) were anesthetized with isoflurane and placed in a stereotaxis frame. Holes were

drilled in the skull above the lateral amygdala [AP = -1.3, ML = +/-3.3, V = -4.8 from bregma according to previous methods³⁰]. Bilateral injections of WT, S40A, or control (p1005+ vector without CREB) HSV (1.5 μ l) were delivered through a Hamilton syringe over 25 min. The syringe was left in place for an additional 10 min prior to retraction. Mice were trained 3 days after the injections.

Training: Mice were placed into a conditioning chamber and, after 2 min, a tone (85 dB, 2000 Hz) was played for 30 s and co-terminating with a footshock (2 s, 0.75 mA). This protocol was chosen because it afforded robust yet non-ceiling levels of freezing. Immediately following or 2 h after training, mice were administered 150 mg kg⁻¹ intraperitoneal anisomycin (Sigma) or saline where indicated.

Conditioning: After 30 min, 2 h, or 24 h, mice were placed into a new cage. After 3 min, a tone (85 dB, 2000 Hz) was played continuously for 3 min. The mice were recorded and monitored for freezing (defined as no movement except breathing) every 5 s during the first 3 min (pre-tone freezing) and the last 3 min (post-tone freezing) by two independent observers, one of whom was blind to the experimental conditions. The percentage freezing was calculated as the mean from both observers divided by the total number of observations. No significant differences were measured in pre-tone freezing scores across all experiments. Following conditioning, mice were perfused with 4% PFA. The brains were embedded in 2% agarose, cut into 50 μ m sections with a vibratome (Leica VT1000s), and imaged for GFP to confirm the correct injection site.

Quantification of CREB glycosylation levels after auditory fear conditioning. Mice were placed into a conditioning chamber. After 2 min, a tone (85 dB, 2000 Hz) was

played for 30 s and co-terminated with a footshock (2 s, 0.75 m). After an additional 2 min, the above sequence was repeated. Control mice were subjected to the above sequence without the shock. Mice were placed back in their transport cage for 15 min, after which they were quickly euthanized with an overdose of isoflurane and decapitated. Brains were removed, the amygdala dissected on ice, and the samples processed for chemoenzymatic labeling as described above.

Statistics. *P* values were calculated from Student's paired t-test when comparing within groups and from Student's unpaired t-test when comparing between groups. ANOVA was used to analyze *in vivo* data. All calculations were performed using the program Excel.

References

1. Hart, G.W., Housley, M.P. & Slawson, C. Cycling of *O*-linked beta-*N*-acetylglucosamine on nucleocytoplasmic proteins. *Nature* **446**, 1017-22 (2007).
2. Rexach, J.E., Clark, P.M. & Hsieh-Wilson, L.C. Chemical approaches to understanding *O*-GlcNAc glycosylation in the brain. *Nat. Chem. Biol.* **4**, 97-106 (2008).
3. Love, D.C. & Hanover, J.A. The hexosamine signaling pathway: deciphering the "*O*-GlcNAc code". *Sci. STKE* **2005**, re13 (2005).
4. Yang, X. et al. Phosphoinositide signalling links *O*-GlcNAc transferase to insulin resistance. *Nature* **451**, 964-9 (2008).
5. Dentin, R., Hedrick, S., Xie, J., Yates, J., 3rd & Montminy, M. Hepatic glucose sensing via the CREB coactivator CRTC2. *Science* **319**, 1402-5 (2008).
6. Vosseller, K. et al. *O*-linked *N*-acetylglucosamine proteomics of postsynaptic density preparations using lectin weak affinity chromatography and mass spectrometry. *Mol. Cell. Proteomics* **5**, 923-34 (2006).
7. Greengard, P. The neurobiology of slow synaptic transmission. *Science* **294**, 1024-30 (2001).
8. Liu, F., Iqbal, K., Grundke-Iqbal, I., Hart, G.W. & Gong, C.X. *O*-GlcNAcylation regulates phosphorylation of tau: a mechanism involved in Alzheimer's disease. *Proc. Natl. Acad. Sci. USA* **101**, 10804-9 (2004).

9. Yuzwa, S.A. et al. A potent mechanism-inspired *O*-GlcNAcase inhibitor that blocks phosphorylation of tau in vivo. *Nat. Chem. Biol.* **4**, 483-90 (2008).
10. Lonze, B.E., Riccio, A., Cohen, S. & Ginty, D.D. Apoptosis, axonal growth defects, and degeneration of peripheral neurons in mice lacking CREB. *Neuron* **34**, 371-85 (2002).
11. Gau, D. et al. Phosphorylation of CREB Ser142 regulates light-induced phase shifts of the circadian clock. *Neuron* **34**, 245-53 (2002).
12. Carlezon, W.A., Jr. et al. Regulation of cocaine reward by CREB. *Science* **282**, 2272-5 (1998).
13. Pittenger, C. et al. Reversible inhibition of CREB/ATF transcription factors in region CA1 of the dorsal hippocampus disrupts hippocampus-dependent spatial memory. *Neuron* **34**, 447-62 (2002).
14. Kida, S. et al. CREB required for the stability of new and reactivated fear memories. *Nat. Neurosci.* **5**, 348-55 (2002).
15. Lamarre-Vincent, N. & Hsieh-Wilson, L.C. Dynamic glycosylation of the transcription factor CREB: a potential role in gene regulation. *J. Am. Chem. Soc.* **125**, 6612-3 (2003).
16. Finkbeiner, S. et al. CREB: a major mediator of neuronal neurotrophin responses. *Neuron* **19**, 1031-47 (1997).
17. Chrivia, J.C. et al. Phosphorylated CREB binds specifically to the nuclear protein CBP. *Nature* **365**, 855-9 (1993).
18. Rexach, J.E. et al. Quantification of O-glycosylation stoichiometry and dynamics using resolvable mass tags. *Nat. Chem. Biol.* **6**, 645-51 (2010).
19. Zhou, Y. et al. Requirement of TORC1 for late-phase long-term potentiation in the hippocampus. *PLoS One* **1**, e16 (2006).
20. Plath, N. et al. Arc/Arg3.1 is essential for the consolidation of synaptic plasticity and memories. *Neuron* **52**, 437-44 (2006).
21. Egan, M.F. et al. The BDNF val66met polymorphism affects activity-dependent secretion of BDNF and human memory and hippocampal function. *Cell* **112**, 257-69 (2003).
22. Wayman, G.A. et al. Activity-dependent dendritic arborization mediated by CaM-kinase I activation and enhanced CREB-dependent transcription of Wnt-2. *Neuron* **50**, 897-909 (2006).
23. Ohshima, T. et al. Targeted disruption of the cyclin-dependent kinase 5 gene results in abnormal corticogenesis, neuronal pathology and perinatal death. *Proc. Natl. Acad. Sci. USA* **93**, 11173-8 (1996).
24. Fleischmann, A. et al. Impaired long-term memory and NR2A-type NMDA receptor-dependent synaptic plasticity in mice lacking c-Fos in the CNS. *J. Neurosci.* **23**, 9116-22 (2003).
25. Aguado, F. et al. The CREB/CREM transcription factors negatively regulate early synaptogenesis and spontaneous network activity. *J. Neurosci.* **29**, 328-33 (2009).
26. Shafi, R. et al. The *O*-GlcNAc transferase gene resides on the X chromosome and is essential for embryonic stem cell viability and mouse ontogeny. *Proc. Natl. Acad. Sci. USA* **97**, 5735-9 (2000).
27. Tucker, K.L., Meyer, M. & Barde, Y.A. Neurotrophins are required for nerve growth during development. *Nat. Neurosci.* **4**, 29-37 (2001).

28. Viosca, J., Lopez de Armentia, M., Jancic, D. & Barco, A. Enhanced CREB-dependent gene expression increases the excitability of neurons in the basal amygdala and primes the consolidation of contextual and cued fear memory. *Learn. Mem.* **16**, 193-7 (2009).
29. Zhou, Y. et al. CREB regulates excitability and the allocation of memory to subsets of neurons in the amygdala. *Nat. Neurosci.* **12**, 1438-43 (2009).
30. Han, J.H. et al. Neuronal competition and selection during memory formation. *Science* **316**, 457-60 (2007).
31. Cox, L.J., Hengst, U., Gurskaya, N.G., Lukyanov, K.A. & Jaffrey, S.R. Intra-axonal translation and retrograde trafficking of CREB promotes neuronal survival. *Nat. Cell. Biol.* **10**, 149-59 (2008).
32. Zhou, Z. et al. Brain-specific phosphorylation of MeCP2 regulates activity-dependent Bdnf transcription, dendritic growth, and spine maturation. *Neuron* **52**, 255-69 (2006).
33. Zhang, F. et al. Lentiviral vectors containing an enhancer-less ubiquitously acting chromatin opening element (UCOE) provide highly reproducible and stable transgene expression in hematopoietic cells. *Blood* **110**, 1448-57 (2007).
34. Clark, P.M. et al. Direct in-gel fluorescence detection and cellular imaging of O-GlcNAc-modified proteins. *J. Am. Chem. Soc.* **130**, 11576-7 (2008).
35. Hansen, B.T., Jones, J.A., Mason, D.E. & Liebler, D.C. SALSA: a pattern recognition algorithm to detect electrophile-adducted peptides by automated evaluation of CID spectra in LC-MS-MS analyses. *Anal. Chem.* **73**, 1676-83 (2001).
36. Khidekel, N., Ficarro, S.B., Peters, E.C. & Hsieh-Wilson, L.C. Exploring the O-GlcNAc proteome: direct identification of O-GlcNAc-modified proteins from the brain. *Proc. Natl. Acad. Sci. USA* **101**, 13132-7 (2004).
37. Li, S., Zhang, C., Takemori, H., Zhou, Y. & Xiong, Z.Q. TORC1 regulates activity-dependent CREB-target gene transcription and dendritic growth of developing cortical neurons. *J. Neurosci.* **29**, 2334-43 (2009).
38. Fan, X., Lamarre-Vincent, N., Wang, Q. & Struhl, K. Extensive chromatin fragmentation improves enrichment of protein binding sites in chromatin immunoprecipitation experiments. *Nucleic Acids Res.* **36**, e125 (2008).
39. Wearne, S.L. et al. New techniques for imaging, digitization and analysis of three-dimensional neural morphology on multiple scales. *Neuroscience* **136**, 661-80 (2005).